Palaeogeography, Palaeoclimatology, Palaeoecology 615 (2023) 111447

Contents lists available at ScienceDirect

Palaeogeography, Palaeoclimatology, Palaeoecology

journal homepage: www.elsevier.com/locate/palaeo

Agulhas leakage extension and its influences on South Atlantic surface water hydrography during the Pleistocene

B. Nirmal [a], K. Mohan [b,*], Aradhna Tripati [c], Beth A. Christensen [d], P. Graham Mortyn [e], David De Vleeschouwer [f], M. Prakasam [g], K. Saravanan [b]

[a] School of Advanced Sciences, Vellore Institute of Technology, Chennai 600127, India
[b] School of Civil Engineering, Vellore Institute of Technology, Chennai 600127, India
[c] Departments of Earth, Planetary, and Space Sciences, Department of Atmospheric and Oceanic Sciences, Institute of the Environment and Sustainability, University of California, Los Angeles 90095, USA
[d] Department of Environmental Science, School of Earth and Environment, Rowan University, Glassboro, NJ, USA
[e] Institute of Environmental Science and Technology (ICTA) and Department of Geography, Universitat Autònoma de Barcelona, 08193 Bellaterra, Barcelona, Spain
[f] Institute of Geology and Paleontology, University of Münster, Corrensstr 24, 48149 Münster, Germany
[g] Wadia Institute of Himalayan Geology, 33, G. M. S. Road, Dehradun 248001, India

ARTICLE INFO

Editor: Prof. M Elliot

Keywords:
Pleistocene
Agulhas leakage fauna
Subtropical Convergence
Deglacial warming
Oceanic teleconnections

ABSTRACT

The inter-ocean transfer of warm and salty water through the Agulhas leakage is regarded as a significant factor influencing the South Atlantic's surface and intermediate water hydrography. To evaluate the extension of Agulhas leakage for the past 1.2 Ma, planktonic foraminiferal assemblage from Ocean Drilling Program Hole 1088B, within the vicinity of AL, and Hole 1090B, located south of the significant Agulhas retroflection region, were generated. The Hole 1088B shows higher abundance of tropical and sub-tropical assemblage. The combination of *Globigerinoides ruber, Trilobatus sacculifer, Globigerinoides conglobatus* and *Globorotalia menardii* has previously been defined as the Agulhas leakage fauna [ALF]. The pulse-like amplification of the ALF record at major glacial-interglacial transitions indicates these were periods of strengthened Agulhas leakage with subsequent shedding of Agulhas rings and filaments as far as ~41°S. From ~450 ka, the frontal zone exhibits strong ALF variations with evident increase at glacial-interglacial transitions of Marine Isotopic Stages (MIS) 12, 10, 8 and 6, suggesting vigorous eddy mixing and a shift in the leakage zone towards the subantarctic waters. The migration of the Subtropical Convergence and *Neogloboquadrina pachyderma (s)* coiling ratios during these glacial-interglacial transitions supports the southward expansion of Agulhas leakage. The ALF record is supported by the $\delta^{18}O$ record of *Globigerina bulloides* from hole 1088B, which identify a major anomaly at MIS 10, with depleted $\delta^{18}O$ values towards the glacial termination. Simultaneously, the results from Hole 1090B show restricted presence of tropical-subtropical assemblage with their appearance reported only at glacial-interglacial transitions of the MIS 16, 12, 10 and 8. The curtailed ALF index and dominance of the subpolar species *N. pachyderma (s)* indicate the termination of Agulhas leakage before reaching the Subantarctic zone. The ODP sites chosen for the study reveal the intensification of Agulhas leakage and southward shift of the major leakage zone into the subantarctic zone during the Pleistocene glacial-interglacial transitions.

1. Introduction

The Agulhas current is a prominent warm water mass in the western boundary of the Indian Ocean and it flows southward parallel to the South East coast of Africa. On reaching the Cape Basin, it experiences retroflection with zero wind stress curl (Beal et al., 2011) by which the larger part of the water mass moves back to the Indian Ocean. At the same time, the separated rings and filaments transport the Agulhas leakage (AL) water into the South Atlantic (Lutjeharms, 1996; de Ruijter et al., 1999). This incoming subtropical AL water mass is much warmer than the surrounding surface waters of the South Atlantic. Thus, the AL interlinks the upper layer waters of both oceans and thereby functions as an interbasin circulation (Speich et al., 2002), which plays a fundamental role in changing the surface hydrography of the South Atlantic

* Corresponding author.
E-mail address: mohan.kuppusamy@vit.ac.in (K. Mohan).

https://doi.org/10.1016/j.palaeo.2023.111447
Received 5 September 2022; Received in revised form 5 January 2023; Accepted 8 February 2023
Available online 13 February 2023
0031-0182/© 2023 Elsevier B.V. All rights reserved.

while facilitating the Atlantic Meridional Overturning Circulation (AMOC). The major contribution to AL is from the Indonesian Throughflow (ITF, 45%) and Tasman Leakage (TL, 30%; Durgadoo et al., 2017). The former flows westward from the Pacific to the Indian Ocean to join a Southern Hemisphere supergyre circulation that connects all the ocean basins (Schott et al., 2009). Model simulations suggest about 90% of ITF waters reach the Agulhas current and exit to the South Atlantic in the upper 1500 m of water column (Durgadoo et al., 2017; Zhang et al., 2019). This warm water route brings fresh surface water and salty intermediate water to the South Atlantic through the AL (Le Bars et al., 2013; Durgadoo et al., 2017). The TL originates from south of Australia and flows westward along the Subtropical Front (STF) and joins the Agulhas current via the south-east Madagascar current (Speich et al., 2002). More than half of water retroflects but TL contributes to AL through intermediate depths (Durgadoo et al., 2017). Of all the various inter-ocean transfers, the AL through the South Atlantic modulates the global ocean circulation balance by replenishing heat and salt to the North Atlantic, thereby also modulating the strength of the AMOC (Beal et al., 2011). New observations suggest that AL is coupled with the strength of the ITF, intensification of Asian monsoons and the strength of the South Indian sub-tropical gyre (Gordon et al., 2008; Beck et al., 2018; Petrick et al., 2019). The atmosphere and ocean teleconnections are significant at oceanic gateways such as the Agulhas corridor.

Most paleo AL reconstructions has been studied previously over the centennial and millennial scales from the main leakage zone in the South Atlantic (Peeters et al., 2004; Martínez-Méndez et al., 2010; Caley et al., 2012; Marino et al., 2013). The paleo reconstructions show enhanced leakage and water mass transport during the glacial-interglacial transitions of the Pleistocene. Sea surface temperature, salinity and Agulhas leakage fauna (ALF) are used as promising proxies in identifying the leakage variability and intensity (Peeters et al., 2004; Martínez-Méndez et al., 2010; Caley et al., 2012; Marino et al., 2013; Simon et al., 2013). The ALF, which is a group of tropical / sub-tropical planktonic foraminifera species found at detached Agulhas rings and filaments (Peeters et al., 2004) is regarded as a reliable proxy in tracing the AL intensity into the south Atlantic. The leakage intensity can be altered by many factors such as the velocity and volume of the Agulhas current, Southern Hemisphere westerlies and fluctuations of hydrographic fronts. Of all these factors, the fluctuations of the STF influence the interocean transfer with a northward position of the front acting as a choke point, by blocking the heat and salt transfer through AL (Bard and Rickaby, 2009). The STF is a region of vigorous interaction between atmosphere and ocean circulation with intense AL retroflection eddy mixing south of Africa. A change in the Earth's orbital parameters, the position of westerlies, and solar insolation all exert control on the position of the STF and thereby leakage variability. The enhanced leakage during the interglacials increases the strength of the AMOC and plays a pivotal role in global heat transfer (Peeters et al., 2004; Bard and Rickaby, 2009; Beal et al., 2011; Caley et al., 2012).

Here we present a planktonic foraminiferal record from the vicinity of the STF and within the Subantarctic Zone (SAZ). Ocean Drilling Progam (ODP) Sites 1088 and 1090 along with previously studied Site 1089 (Cortese et al., 2004) are optimally located to observe the interaction between AL and the Southern Ocean, and also to monitor major shifts in leakage intensity. Here the mixing of warm, saline spillage with cold, eutrophic sub-Antarctic waters creates an oceanographic divide with variable surface water hydrography. Today these sites are dominated by subpolar and transitional planktonic foraminifera but based on previous studies (e.g., Peeters et al., 2004) it is anticipated that they should vary under different conditions. This study attempts to establish the extent of AL into the SAZ and to identify the leakage termination point. A 1.2 Ma record of planktonic foraminifera proxies was utilized to unveil the late Pleistocene zonal shift in AL, covering the two climatic transitions, the Mid Pleistocene Transition (MPT), ~1.25–0.7 Ma (Elderfield et al., 2012; Diester-Haass et al., 2018) and the Mid Bruhnes Event (MBE), ~0.43 Ma (Barth et al., 2018).

2. Study area

The Pleistocene sediment successions from the two South Atlantic Holes (ODP Leg 177) close to the Agulhas retroflection region were examined for the study (Fig. 1). ODP Hole 1088B was drilled on the Agulhas ridge, (41°8.16′S, 13°33′E, 2082 m water depth) in the vicinity of the modern-day STF (Becquey and Gersonde, 2002). Although proximal to but not within the main AL, Site 1088 provides a record of changes in the STC. Surface waters here are transitional based on the planktonic foraminiferal abundance and SST, and the site remains in the reaches of Agulhas retroflection rings and filaments (Lutjeharms, 1996). The intermediate water depth places the Site 1088 in the boundary between North Atlantic Deep Water (NADW) and upper Circumpolar Deep Water (CPDW) (Reid, 1989). The sediments recovered from Site 1088 are carbonate-rich with low sedimentation rate (0.1 cm/ka) throughout the Pleistocene (Gersonde et al., 1999). The more southerly Hole 1090B, drilled on the South Western flank of the Agulhas ridge, lies in the central SAZ (42°54′S, 8°53′E, 3702 m water-depth), south of the Agulhas retroflection zone. Site 1090 is useful to record changes in the SAZ. This deeper site rests in the mixing zone of lower CPDW and NADW (Reid, 1989) and above the calcium carbonate compensation depth, which ensures preservation of carbonate rich sediments. The site records Pleistocene sedimentation rates of 0.3 cm/ka, which is higher than the intermediate site due to the high opal deposition (Gersonde et al., 1999) and increased terrestrial deposition (Martínez-Garcia et al., 2011) occurring at the subantarctic zone. Both Sites 1088 and 1090 are ideally located south of the prominent Agulhas corridor, which makes this region much more sensitive for large scale changes in leakage intensity or a southern shift in leakage zone.

3. Material and methods

3.1. Age model and stable isotope analysis

The age models for ODP Holes 1088B and 1090B are based on biostratigraphic datums and oxygen isotope stratigraphy. We used the age model calibrated in Nirmal et al., 2021 for Hole 1088B, where shipboard calcareous nannofossils were corroborated with benthic $\delta^{18}O$ data from (Billups, 2002) and age calibration was graphically constructed against the LR04 benthic $\delta^{18}O$ stack (Lisiecki and Raymo, 2005). We also used the age model proposed by Martínez-Garcia et al. (2010) for Hole 1090B.

For this study, we used the *G. bulloides* $\delta^{18}O$ values previously recorded by Nirmal et al. (2021). Overall, 120 samples (57 from 1088B and 63 from 1090B) were measured with a Finnigan MAT 253 plus mass spectrometer linked with an automated Kiel IV carbonate device at Wadia Institute of Himalayan Geology, Dehradun, India. The isotope values were calibrated to the international standard Vienna Pee Dee Belemnite (VPDB) with the IAEA isotopic reference material NBS-18. Merck carbonate was also used as an in-house secondary standard. The external reproducibility was 0.08‰ for the $\delta^{18}O$ analysis.

3.2. Sample processing and foraminiferal census counts

One hundred and forty samples (57 from Hole 1088B and 83 from Hole 1090B) covering 1.2 Ma were processed by following the standard procedures for sample processing and wet sieving (Mohan et al., 2011). Planktonic foraminiferal counts were performed over the >150 μm size fraction, for at least 300–500 specimens per sample. The relative abundance record is then used to obtain the ALF index. The ALF at the southern STF comprised of *Globigerinoides ruber, Trilobatus sacculifer, Globigerinoides conglobatus* and *Globorotalia menardii*, as observed from the study area (Table 1).

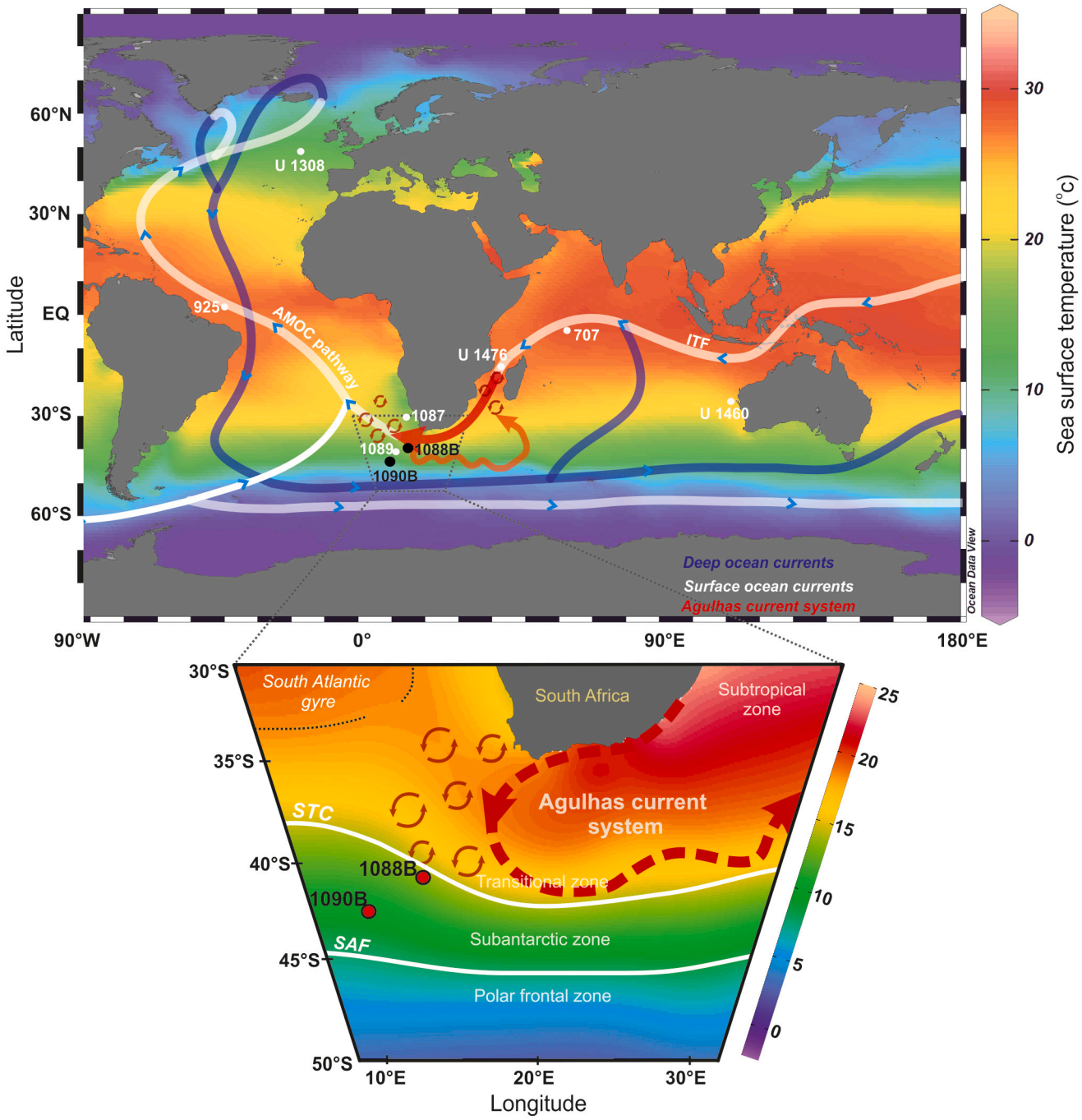


Fig. 1. Location of the study area and global Meridional Overturning Circulation (MOC). The South Atlantic ODP Holes 1088B (within AL) and 1090B (outside of the main AL region) are represented by *Black dots*. Other Sites (*white dots*) along the path of MOC are included for comparison. The prominent, modern Agulhas zone is shown by the thick red line with red circles indicating the warm Agulhas eddies and rings. The oceanic connection between ITF (Indonesian Throughflow), AL (Agulhas leakage) and AMOC (Atlantic Meridional Overturning Circulation) is shown (Modified from Broecker, 1991 and Rahmstorf, 2002). (For interpretation of the references to colour in this figure legend, the reader is referred to the web version of this article.)

3.3. Principal components and foraminiferal index

The relative abundance of planktonic species is taken as the primary input for the PCA factor analysis. The analysis was performed for Holes 1088B and 1090B using the software STATISTICA, version 10.0 (Tables 1, 2). The factor loadings present the correlation between different species and samples (Kucera, 2003). The factors were chosen with eigenvalues >1, and the scores were rotated by the Varimax method to interpret environmental parameters (Fig. 2).

3.3.1. Relative subtropical convergence (STC) index

The latitude of STC migration is crucial for the AL to reach the South Atlantic. It also determines the strength and displacement of Southern Hemisphere westerlies (Bard and Rickaby, 2009). Peeters et al. (2004) developed an index for this study area using the relative abundance of transitional planktonic foraminifera. Subtropical to transitional waters exists at the STC and the location of Hole 1088B (~ 41°S) is optimal to derive the STC index: *G. truncatulinoides* are found in abundance north of the STC while transitional species *G. inflata* and *N. pachyderma (dex.)* dominate the assemblages to the south of the STCSTC index =

Table 1
Varimax factor loadings, 1088B, South Atlantic.

Species name	Factor -1	Factor -2	Factor -3	Factor -4
Globigerina bulloides	0.312034	0.275422	**0.750619**	0.144094
Globigerinita glutinata	0.239875	0.317389	0.492279	0.221169
Globigerinoides conglobatus	**0.829511**	0.029922	0.024323	0.209100
Globigerinoides ruber	**0.765890**	0.245871	0.050567	0.225735
Trilobatus sacculifer	**0.921452**	−0.071687	−0.062499	0.140845
Globorotalia crassaformis	0.067700	0.175054	−0.090081	**0.813915**
Globoconella inflata	0.331750	0.012871	**0.632269**	0.439716
Globorotalia menardii	**0.844009**	0.058888	0.147162	−0.141287
Globorotalia truncatulinoides	0.540129	0.024391	0.300637	0.250125
Neogloboquadrina dutertrei	0.246889	0.589598	−0.031369	−0.126890
Neogloboquadrina pachyderma (sin.)	−0.045222	**0.880681**	0.117020	0.127778
Turborotalia quinqueloba	−0.154709	**0.910756**	0.099204	0.071230
Orbulina universa	0.479552	0.130197	−0.630181	0.067584
Neogloboquadrina pachyderma (dex.)	0.564082	−0.502563	0.268082	−0.223459
Cumulative variance (%)	**33**	**54**	**64**	**72**

Factor loadings of PCA (Varimax-rotated). The scores represent species loading. Species marked in bold combine to form Agulhas leakage fauna.
Factor − 1, Agulhas leakage fauna (depth habitat - mixed layer, 0–250 m).
Factor − 2, Species representing subantarctic to polar zone (depth habitat, 0–200 m); **G. inflata* depth habitat, 100–500 m.
Factor − 3, Species indicative for the transitional-subpolar zones (depth habitat, 0–200 m).
Factor − 4, Species indicative of the subtropical to transitional zones (depth habitat, 100–500 m).
Depth habitat from plankton tows in Atlantic sector of Southern Ocean (Mortyn and Charles, 2003).

Table 2
Varimax factor loadings, 1090B, South Atlantic.

Species name	Factor -1	Factor -2
Globigerina bulloides	**0.889997**	0.002744
Globigerinita glutinata	**0.837150**	0.079330
Globigerinita parkerae	−0.074839	−0.159207
Globigerinita uvula	0.286006	0.081068
Globigerinoides ruber	0.014096	**0.964826**
Trilobatus sacculifer	0.062923	**0.951153**
Globorotalia crassaformis	0.112024	−0.069772
Globoconella inflata	**0.828621**	0.158710
Globoconella puncticulata	−0.555377	−0.314827
Globorotalia truncatulinoides	0.544498	0.625942
Neogloboquadrina pachyderma (sin.)	**−0.738409**	0.019665
Turborotalia quinqueloba	0.322214	0.158999
Orbulina universa	0.160695	0.162364
Neogloboquadrina pachyderma (dex.)	0.008631	−0.015196
Cumulative variance (%)	**84**	**95**

Factor loadings of PCA (Varimax-rotated). The scores represent species loading. Species marked in bold combine to form ALF.
Factor − 1, positive loading represents species of transitional to subpolar zone (depth habitat, 0–200 m); **G. inflata* depth habitat, 100–500 m. Negative loading indicate species of subantarctic to polar zone (depth habitat, 0–200 m).
Factor − 2, Agulhas leakage fauna (depth habitat - mixed layer, 0–250 m).
Depth habitat from plankton tows in Atlantic sector of Southern Ocean (Mortyn and Charles, 2003).

ratio of (*G. truncatulinoides*)/((*N. pachyderma*(dex.) + *G. inflata* + *G. truncatulinoides*)).

3.3.2. *N. pachyderma coiling ratio*

The coiling ratio in *N. pachyderma* is used by micropaleontologists to reconstruct paleoceanographic and environmental changes (Darling et al., 2006). *Neogloboquadrina pachyderma* in subantarctic waters shows two distinctive coiling patterns, which are linked with surface ocean temperature. The left-coiling morphotype of *N. pachyderma* is abundant in polar waters while the right-coiling morphotype prefers more transitional and temperate waters (Darling et al., 2006; Itaki, 2016). At the South Atlantic STC zone, the left-coiling variant dominates (> 95%) with aberrant right coiling morphotypes (< 5%). The frontal characteristics of the study area and drastic temperature change at the STC may have regulated the mixing of these morphotypes in the study area. The ratio of dextral to sinistral variants of *N. pachyderma* from the Hole 1088B is used as a paleoceanographic proxy in the South Atlantic.

4. Results

4.1. Planktonic foraminifera records from the Subtropical Convergence (STC), ODP Hole 1088B

The relative abundance of major planktonic foraminifera from Hole 1088B are used to examine the surface ocean changes in the STC zone. The species relative abundance is utilized to perform factor analysis (PCA) which condenses the data to various environmental preferences. Four factors were retained with eigenvalues >1, which together explained 72% of variance in the dataset (Table 1). The factor loadings >0.60 were grouped as species residing in similar environments (Fig. 2). We observed glacial-interglacial variations in the foraminiferal assemblage after the onset of the MPT (~1250 ka), which indicates significant surface water changes at the STC during the late Pleistocene. The glacial stages after the MPT show higher abundance in Polar assemblage (*N. pachyderma* and *T. quinqueloba*) (Tolderlund, 1971; Schiebel and Hemleben, 2017) reflecting cold and high productive waters, but the maximum abundances (>40%) at MIS 12 and 6 may indicate the northward displacement of ACC fronts and intrusion of cold Antarctic surface waters into the STC zone (Fig. 3a). The transitional group (*G. bulloides, G. inflata* and *G. glutinata*) that represents subpolar to transitional assemblage in the South Atlantic (Tolderlund, 1971; Schiebel and Hemleben, 2017) indicates glacial-interglacial fluctuations (Fig. 3b). The subtropical assemblage (*G. crassaformis, G. truncatulinoides* and *N. dutertrei*) increases in abundance at the glacial transitions after the inception of the MBE (~430 ka; Fig. 3c). The fourth group (Factor 1) represents ALF (*G. ruber, T. sacculifer, G. conglobatus* and *G. menardii)*, and occurs in pulse-like episodes at the major glacial - interglacial terminations between 1.2 and 0.5 Ma (Fig. 3d). After the intensification of the MBE, the ALF exhibits strong glacial-interglacial variations with evident increases at glacial terminations of MIS 12, 10, 8 and 6.

The planktonic $\delta^{18}O$ records were used to corroborate the ALF index, but lacks high resolution to correlate at every glacial termination. Pleistocene core sediments at the site were depleted and any high resolution study is unattainable. The $\delta^{18}O$ values range from 3.75 to 1.90‰ for the last 1.2 Ma and are consistent with what has previously been reported for this location (Hodell et al., 2003). The isotope record of *G. bulloides* identifies an anomaly at MIS 10, suggesting near interglacial $\delta^{18}O$ values towards the glacial termination. Though the record is of low resolution, MIS 10 at Hole 1088B represents the most depleted $\delta^{18}O$ signal during the late Pleistocene (Fig. 5g).

4.2. Planktonic foraminiferal records from the Subantarctic Zone (SAZ), ODP Hole 1090B

The relative abundance of major planktonic foraminifera from ODP Hole 1090B were used to examine the surface ocean changes in the SAZ. The PCA factor analysis retains four factors with eigenvalues >1, but the first two factors explain 95% of the variance in the planktonic abundance (Table 2). Factor 1 remains the most important with sub-polar to transitional assemblage (*G. bulloides, G. inflata* and *G. glutinata*) with positive correlation and polar species *N. pachyderma* showing a negative

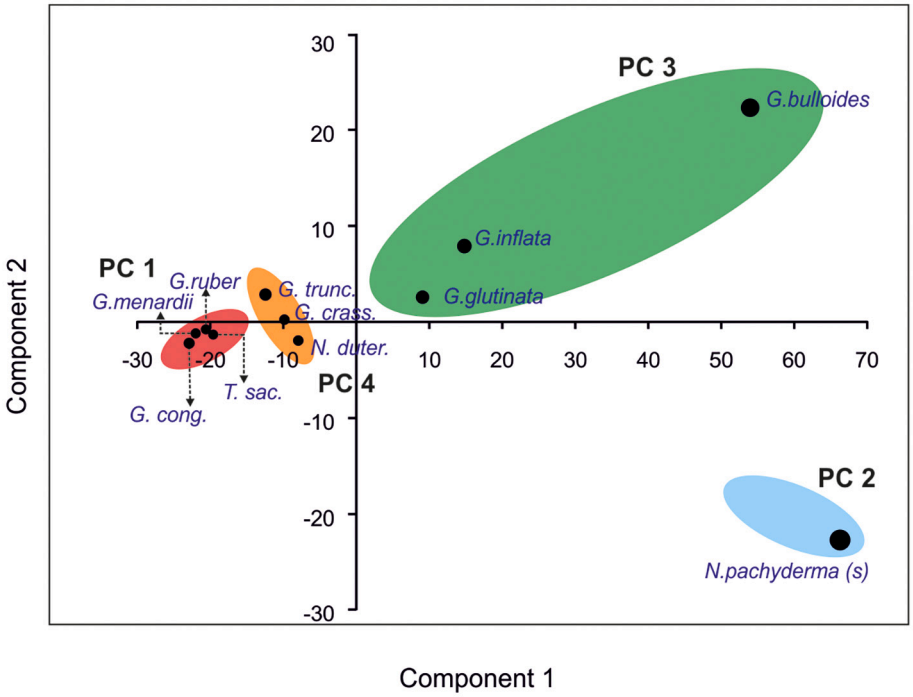


Fig. 2. Principal component analysis. Scatter plot of PC 1 / PC 2 of planktonic foraminifera from ODP Hole 1088B. Species specific environmental conditions and their relationship is represented. The planktonic foraminifera are classified into polar (*blue*), transitional (*green*), sub-tropical to transitional (*orange*) and tropical to sub-tropical (*red*). (For interpretation of the references to colour in this figure legend, the reader is referred to the web version of this article.)

correlation. *Neogloboquadrina pachyderma (s.)* almost individually dominates both the glacial and interglacial assemblage from 1.2 to 0.5 Ma with 60–80% abundance recorded during major glacial intervals (Fig. 3a). This suggests the northward migration of the STC and the subsequent expansion of cold water masses at the site. These migrations and expansions were even more marked during pre-MBE times, as glacials (and interglacials as well) had even higher amounts of polar assemblage during that time interval. After the MBE the interglacial intervals indicate higher abundance of transitional assemblage (Fig. 3b) but is often dominated by *N. pachyderma (s.)*. The subtropical group (*G. crassaformis* and *G. truncatulinoides*; Fig. 3c) and ALF (*G. ruber* and *T. sacculifer)* are restricted during the MPT but suggest a period of surface water change with slight yet vital occurrence at glacial transition of MIS 10 (Fig. 3d). The planktonic $\delta^{18}O$ record from this central SAZ site varies from 4.00 to 2.5‰ (Fig. 5f) and agrees with previous studies (Martínez-Garcia et al., 2010; Venz and Hodell, 2002). The enriched $\delta^{18}O$ measurements compared to STC bound Site 1088 point to predominant cold Antarctic surface water conditions south of the STC.

5. Discussion

5.1. Agulhas leakage export to the South Atlantic

The four factor scores retained from the STC bound site groups plannktonic foraminifera with similar ecology together. Factor 1 was statistically significant in interpreting ALF and show a negative correlation ($r = -0.61$) between ALF and $\delta^{18}O$ signature during post MBE glacial transitions (Fig. 4). In the modern South Atlantic, ALF comprise typical tropical to subtropical species present in the detached Agulhas rings (Peeters et al., 2004). The presence of these tropical - subtropical species is reported at various sites north of the modern day STC during the late Pleistocene, such as MD96–2081 (Peeters et al., 2004); MD 96–2080 (Martínez-Méndez et al., 2010); ODP 1087 (Caley et al., 2012) (Supplementary fig. 1). The AL contribution to the STC is traced by the presence of ALF along with warm and saline surface waters reaching ODP Site 1088. The ALF index from Sites 1088 and 1090 may not be sensitive to minor changes but to major variations in the AL. The ALF record is subdued during the MPT (1.2–0.7 Ma; Fig. 5d), a period of shift in intensity of glacial cycles (Ford and Chalk, 2020). This interval is characterized by enriched glacial $\delta^{18}O$ values and relatively cold SST in the South Atlantic (Fig. 5g, e). The ALF are depleted at the SAZ, at least judging from the rare occurrence of subtropical to tropical species recorded at Hole 1090B (Fig. 5c). The ALF index hints at the termination of AL waters beyond the STC zone, and a northward migration of fronts for most of the MPT indicated by the STC index (Fig. 5b). Previous studies report that southern sourced waters extensively dominated during the MPT (Farmer et al., 2019) resulting in subsequent northward excursion of SAZ. Southern Hemisphere summer insolation minima at this time period point to expanded Antarctic Sea ice (Raymo et al., 2006) which increased the water column stratification at SAZ (Hasenfratz et al., 2019).

By MIS 18 (~0.7 Ma) the shift in glacial periodicity to 100 kyr cycles was complete. Deglacial warming was prominent at the STC during the transitions of MIS 18 and 16 (Fig. 5g). At these transitions, the ALF index at Hole 1088B was coupled with the depleted $\delta^{18}O$ values of *G. bulloides*. The ALF index from Hole 1090B suggests the SAZ remained out of the reaches from AL even after the MPT (0.7–0.45 Ma). The data are supported by the huge difference in sea surface temperature at both sites (Fig. 5e). Both transitions of MIS 18 and 16 suggest the southward shift of the STC zone, suggesting the export of AL as far as modern day STC (41°S).

5.1.1. Post MBE super-interglacials

After the inception of the MBE (~0.43 Ma), the South Atlantic saw an intensification of glacial-interglacial variability. The influence of AL strengthened at Hole 1088B based on the proxy records (ALF index, surface $\delta^{18}O$ and SST records) and the relationship between Factor 1 and $\delta^{18}O$, invigorated after the MBE (Fig. 4). The ALF index from the STC bound site increases during the glacial – interglacial transitions of MIS 12, 10 and 8 (Fig. 5d). The $\delta^{18}O$ and SST record from the studied sites as well as adjacent Sites ODP 1087 (Caley et al., 2012; Petrick et al., 2018) and 1089 (Cortese et al., 2004) show the deglacial warming trend at

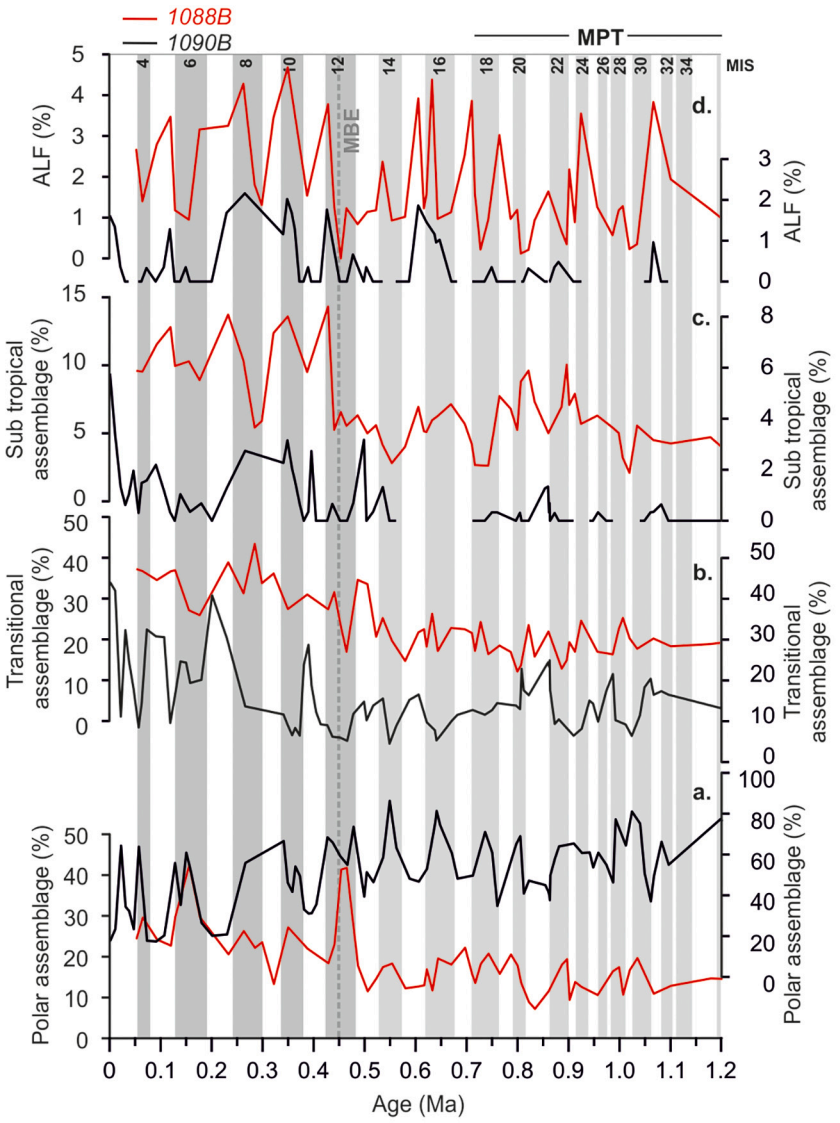


Fig. 3. The relative abundance of planktonic foraminifera from ODP Holes 1088B and 1090B over the past 1.2 My. (a) Sub Polar zone (*N. pachyderma (s) and (d), T. quinqiloba*); (b) Transitional zone (1088B - *G. bulloides*, *G. inflata* and *G. glutinata;* 1090B - *G. bulloides*, *G. inflata, G. glutinata and G. puncticulata*); (c) Sub-Tropical to transitional (1088B - *G. truncatulinoides, G. crassaformis* and *N. dutertrei;* 1090B - *G. truncatulinoides* and *G. crassaformis*); (d) ALF % (1088B - *G. ruber, T. sacculifer, G. conglobatus* and *G. menardii;* 1090B - *G. ruber* and *T. sacculifer*). The grey bars represent the Marine Isotopic stages (Lisiecki and Raymo, 2005).

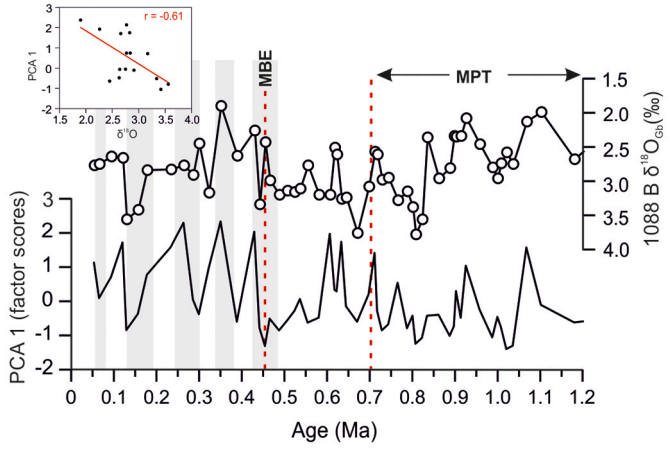


Fig. 4. Relationship between Factor 1 scores and the $\delta^{18}O$ signature of *G. bulloides* (VPDB) from ODP Hole 1088B during the late Pleistocene.

these transitions. This intensification in AL may be the cause of super-interglacials after MBE (Turney and Jones, 2010) and thereby strengthening of the AMOC (Peeters et al., 2004; Caley et al., 2012).

Polar assemblage started dominating the glacial intervals while glacial-interglacial transitions were marked by the AL export. The transition of MIS 10 signifies an anomaly in the $\delta^{18}O$ record of *G. bulloides* at Hole 1088B, the lowest values reported at the site (Fig. 5g). A similar SST increase at MIS 10 is reported from an adjacent Site, ODP 1089 (Cortese et al., 2004) while southern Site 1090 shows the maximum ALF index during the late Pleistocene (Fig. 5c). This could explain a southward zone shift in AL, infiltrating the STC surface waters during the deglacial warming of MIS 12, 10 and 8. The southern shift of STC and the shift in westerlies (Martínez-Garcia et al., 2011) during these intervals also support the southern shift in the leakage zone. The glacial - interglacial transitions after MBE record an increase in dextral *N. pachyderma* abundance signifying warmer surface water conditions. Our ALF index clearly represents a choke point of AL at the SAZ (ODP 1090), with an imperceptible occurrence of Tropical-Sub-tropical planktonic assemblage. The pattern of ALF index and planktonic assemblage suggests the extension of AL as far as ~41°S (modern day STF). The subantarctic surface waters remain independent of this interocean transfer other than a period of major southern shift in the leakage zone.

5.2. *Response of the STC zone to late Pleistocene oceanic teleconnections*

The shift to 100 ky cycles by ~0.7 Ma saw severe glacial conditions

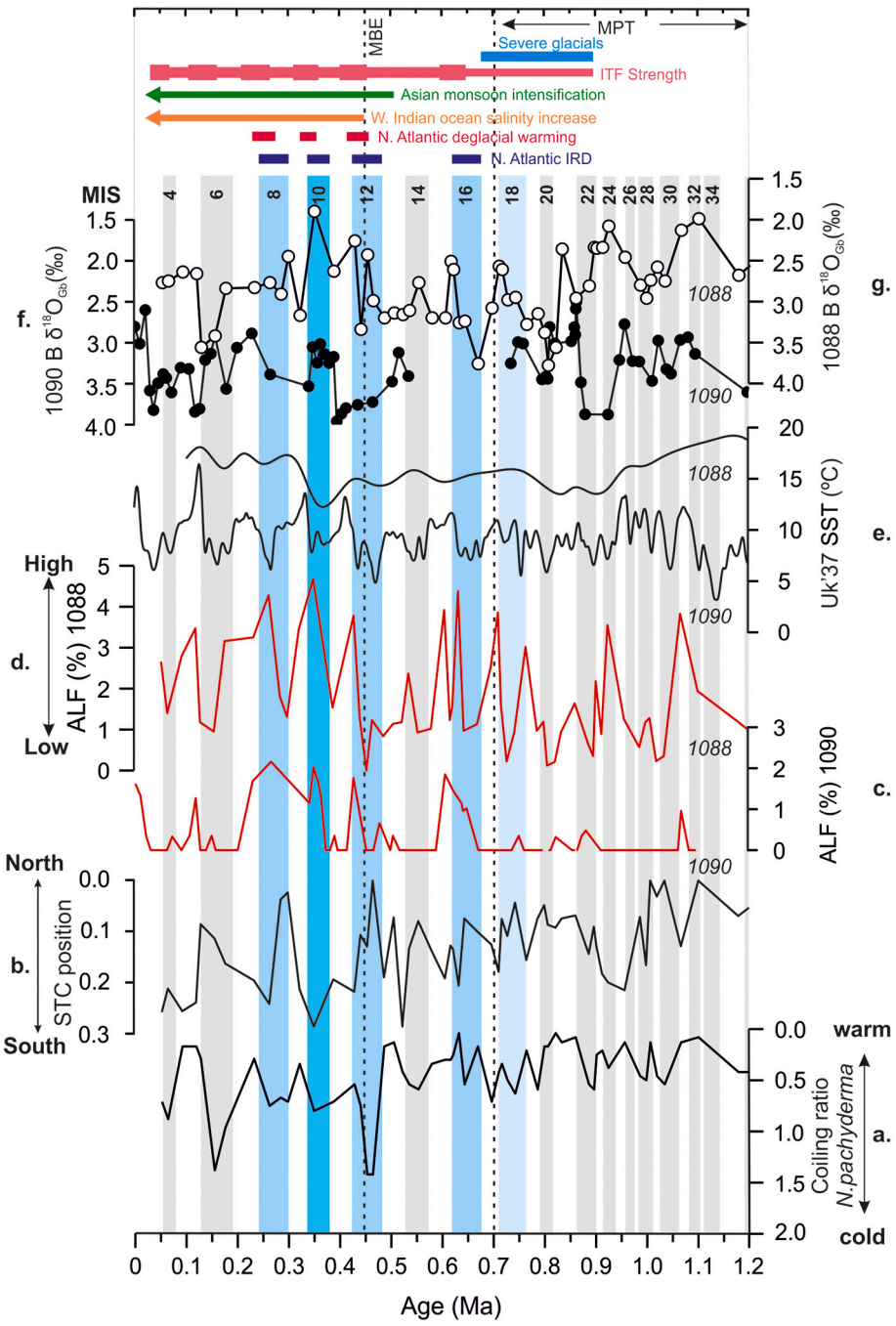


Fig. 5. Comparison of the 1.2 Ma relative abundance record of ALF index from South Atlantic sector with (a) Coiling ratio between dextral and sinistral *N. pachyderma*, ODP 1088B; (b) STC position derived from planktonic foraminiferal abundance (1088B); (c) 1090B ALF index; (d) 1088B ALF index; (e) SST values from ODP Site 1088 (Herbert et al., 2016) and ODP Site 1090 (Martínez-Garcia et al., 2010); (f) The $\delta^{18}O$ values of *G. bulloides* (VPDB) from ODP Hole 1090B (Nirmal et al., 2021); (g) The $\delta^{18}O$ values of *G. bulloides* (VPDB) from ODP Hole 1088B (Nirmal et al., 2021). The grey bars represent the Marine Isotopic stages (Lisiecki and Raymo, 2005), and the blue shading represents MIS stages indicating deglacial warming. Regional and Global events – Severe glacial conditions from MIS 22 - MIS 16 (Ford and Chalk, 2020); ITF strength (Holbourn et al., 2011: Petrick et al., 2019); Summer Monsoon intensification from 0.5 Ma (Sun et al., 2010; Beck et al., 2018); W. Indian Ocean high salinity (Nuber et al., 2021); Equitorial and North Atlantic deglacial warming / AMOC strength (Diester-Haass et al., 2018); North Atlantic IRD and HE (Hodell et al., 2008). (For interpretation of the references to colour in this figure legend, the reader is referred to the web version of this article.)

followed by weaker interglacials (Ford and Chalk, 2020). Before ~0.7 Ma, the weak signals in ALF index at the STC site indicated restricted leakage into the South Atlantic. During this period the oceanic teleconnection was weak with large glacial ice build-up in the Northern Hemisphere, a decrease in ITF intensity, reduced Asian summer monsoon, curtailed AL, the extension of Antarctic Sea ice and weakened meridional overturning circulation (Petrick et al., 2019). By the end of MPT (~0.7 Ma) the ALF index shows signs of deglacial warming at Hole 1088B. This MIS 16 deglacial warming signal is also visible in the SST record from the west coast of Australia (IODP Site U1460, water depth, 215 m), which is a proxy record for enhanced ITF strength (DiNezio et al., 2018; Petrick et al., 2019). As the ITF strengthens it moves westward and intensifies the South Equatorial Current (SEC) and the southern Indian sub-tropical gyre (Le Bars et al., 2013). Modern observations link Asian monsoons with the strength of the Indian Ocean sub-tropical high (Beck et al., 2018). A late Pleistocene Asian monsoon record from Chinese Loess (Sun et al., 2010; Beck et al., 2018) shows an increase in monsoon intensity around 0.5 Ma. Also, the interglacial intervals after MBE record intensified Asian monsoons and is regarded as positive feedback to ITF strength. From the Transition of MIS 12, intensified deglacial warming and high salinity are reported from western Indian Ocean Site U1476 (Nuber et al., 2021). This indicates the addition of ocean salinity to the Agulhas corridor from Indian Ocean surface waters. The oceanic connection is well documented when the SST record and ALF index from Agulhas corridor and Hole 1088B (STC zone) indicate warming at the transitions of MIS 16, 12, 10 and 8. The MIS 12, 10 and 8 transitions show the maximum abundance of ALF index at 1088B and 1090B are coupled with the increase in ITF, and the related feedback system. The MIS 10 anomaly visible at Sites 1088 and 1089 (this study; Cortese et al., 2004) suggests this as the period of

strongest feedback which occurred at the STC during the Pleistocene. At MIS 10, the STC expanded southwards, invigorating strong AL towards the SAZ. The increased AL and eddy circulation at transitions of MIS 12, 10 and 8 had in turn supported the northward flow of AMOC. SST records from equatorial Atlantic Site ODP 925 (Bickert et al., 1997; Diester-Haass et al., 2018) and North Atlantic Site 980 (McManus et al., 1999) reveal this northward advection of heat which strengthens the AMOC. By MIS 16 a considerable increase in ice rafted detritus was recorded from North Atlantic IODP Site U1308 (water depth, 3427 m). The observed detrital layers (Hudson strait events) from the North Atlantic site also signify deglacial warming which destabilizes the Laurentide ice sheet. These oceanic teleconnections reveal a feedback loop between intensified AL and meridional overturning circulation across the globe. This could activate a global warmhouse transformation at forthcoming glacial-interglacial transitions just like the unusual MIS 11/10 transition.

6. Conclusions

Planktonic foraminiferal records from two sites in the South Atlantic reveal the influence of AL at the STC and SAZ during the late Pleistocene (1.2 Ma). The factor analysis applied to the foraminiferal census count identifies the tropical-subtropical assemblage as the ALF index. The ALF index from Hole 1088B traces the Agulhas influx into the STC zone at major glacial terminations. The ALF is visible in small pulse like episodes during the MPT, and intensified at terminations of MIS 12, 10 and 8 after the onset of the MBE (~0.43 Ma). At Hole 1090B the ALF index indicates restricted AL into the SAZ and influence of leakage is present only at terminations of MIS 12 and 10. ALF data is combined with the $\delta^{18}O$ record, which identifies an anomaly at MIS 10 with interglacial values towards the glacial terminations. Our proxy records along with previous studies from the South Atlantic suggest the influence of AL extends up to ~41°S in the STC zone. The transitions of MIS 12, 10 and 8 are considered as the peak extension and zone shifting of leakage towards the SAZ based on a southward shift in STC index coupled with increasing abundance of dextral *N.pachyderma*. The super interglacials after MBE show that oceanic teleconnections between the South Atlantic and other ocean basins were intensified. The strongest feedback of oceanic teleconnections at the STC is observed at the deglacial warming of MIS 10. The strength of the ITF, Monsoon intensification and strength of South Indian Ocean sub-tropics are coupled with the energy of Agulhas current and volume of the leakage to the South Atlantic. Deglacial warming and AL accentuate to the meridional overturning circulation strength during the Pleistocene and thereby balancing the global climate.

Declaration of Competing Interest

The authors hereby declare that they have no known competing financial interests or personal relationships that could have appeared to influence the work reported in this paper.

Data availability

Data will be made available on request.

Acknowledgements

We thank the Science and Engineering Research Board (SERB), New Delhi, India for funding this research work (Reference No: SERB/F/8907/2016-17). BN supported by SERB fellowship. The core samples were acquired by KM from the IODP Bremen core repository (request no. #035841IODP and #051341IODP). The authors are grateful to the editor and reviewers for their constructive comments, which helped to improve the publication's quality. The facilities at Geoscience Research Lab, Vellore Institute of Technology, Chennai are also gratefully acknowledged.

Appendix A. Supplementary data

Supplementary data to this article can be found online at https://doi.org/10.1016/j.palaeo.2023.111447.

References

Bard, E., Rickaby, R.E., 2009. Migration of the subtropical front as a modulator of glacial climate. Nature 460 (7253), 380. https://doi.org/10.1038/nature08189.
Barth, A.M., Clark, P.U., Bill, N.S., He, F., Pisias, N.G., 2018. Climate evolution across the mid-brunhes transition. Clim. Past 14 (12), 2071–2087. https://doi.org/10.5194/cp-14-2071-2018.
Beal, L.M., De Ruijter, W.P., Biastoch, A., Zahn, R., Cronin, M., Hermes, J., Lutjeharms, J., Quartly, G., Tozuka, T., Baker-Yeboah, S., Bornman, T., 2011. On the role of the Agulhas system in ocean circulation and climate. Nature 472 (7344), 429. https://doi.org/10.1038/nature09983.
Beck, J.W., Zhou, W., Li, C., Wu, Z., White, L., Xian, F., Kong, X., An, Z., 2018. A 550,000-year record of East Asian monsoon rainfall from 10Be in loess. Science 360 (6391), 877–881. https://doi.org/10.1126/science.aam5825.
Becquey, S., Gersonde, R., 2002. Past hydrographic and climatic changes in the Subantarctic Zone of the South Atlantic-the Pleistocene record from ODP Hole 1090. Palaeogeogr. Palaeoclimatol. Palaeoecol. 182 (3), 221–239. https://doi.org/10.1016/S0031-0182(01)00497-7.
Bickert, T., Curry, W.B., Wefer, G., 1997. Late Pliocene to Holocene (2.6-0 Ma) western equatorial Atlantic deep-water circulation: inferences from benthic stable isotopes. In: Proceedings of the Ocean Drilling Program. Scientific Results 154, pp. 239–253.
Billups, K., 2002. Late Miocene through early Pliocene deep water circulation and climate change viewed from the sub-Antarctic South Atlantic. Palaeogeogr. Palaeoclimatol. Palaeoecol. 185 (3–4), 287–307.
Broecker, W.S., 1991. The great ocean conveyor. Oceanography 4 (2), 79–89.
Caley, T., Giraudeau, J., Malaizé, B., Rossignol, L., Pierre, C., 2012. Agulhas leakage as a key process in the modes of Quaternary climate changes. Proceedings of the National Academy of Sciences 109 (18), 6835–6839. https://doi.org/10.1073/pnas.1115545109.
Cortese, G., Abelmann, A., Gersonde, R., 2004. A glacial warm water anomaly in the subantarctic Atlantic Ocean, near the Agulhas Retroflection. Earth Planet. Sci. Lett. 222 (3–4), 767–778. https://doi.org/10.1016/j.epsl.2004.03.029.
Darling, K.F., Kucera, M., Kroon, D., Wade, C.M., 2006. A resolution for the coiling direction paradox in Neogloboquadrina pachyderma. Paleoceanography 21 (2), 2011. https://doi.org/10.1029/2005PA001189.
de Ruijter, W.D., Biastoch, A., Drijfhout, S.S., Lutjeharms, J.R.E., Matano, R.P., Pichevin, T., Van Leeuwen, P.J., Weijer, W., 1999. Indian-Atlantic interocean exchange: dynamics, estimation and impact. J. Geophys. Res. Oceans 104 (C9), 20885–20910.
Diester-Haass, L., Billups, K., Lear, C., 2018. Productivity changes across the mid-Pleistocene climate transition. Earth Sci. Rev. 179, 372–391. https://doi.org/10.1016/j.earscirev.2018.02.016.
DiNezio, P.N., Tierney, J.E., Otto-Bliesner, B.L., Timmermann, A., Bhattacharya, T., Rosenbloom, N., Brady, E., 2018. Glacial changes in tropical climate amplified by the Indian Ocean. Sci. Adv. 4 (12), 9658. https://doi.org/10.1126/sciadv.aat9658.
Durgadoo, J.V., Rühs, S., Biastoch, A., Böning, C.W., 2017. Indian Ocean sources of Agulhas leakage. J. Geophys.Res.Oceans 122 (4), 3481–3499. https://doi.org/10.1002/2016JC012676.
Elderfield, H., Ferretti, P., Greaves, M., Crowhurst, S., McCave, I.N., Hodell, D., Piotrowski, A.M., 2012. Evolution of ocean temperature and ice volume through the mid-Pleistocene climate transition. Science 337 (6095), 704–709. https://doi.org/10.1126/science.1221294.
Farmer, J.R., Hönisch, B., Haynes, L.L., Kroon, D., Jung, S., Ford, H.L., Raymo, M.E., Jaume-Seguí, M., Bell, D.B., Goldstein, S.L., Pena, L.D., 2019. Deep Atlantic Ocean carbon storage and the rise of 100,000-year glacial cycles. Nat. Geosci. 12 (5), 355–360.
Ford, H.L., Chalk, T.B., 2020. The Mid-Pleistocene Enigma. Oceanography 33 (2), 101–103. https://doi.org/10.5670/oceanog.2020.216.
Gersonde, R., Hodell, D.A., Blum, P., 1999. Leg 177 summary: southern ocean paleoceanography. In: Proc. Ocean DrillProgram Initial Reports, p. 177.
Gordon, A.L., Susanto, R.D., Ffield, A., Huber, B.A., Pranowo, W., Wirasantosa, S., 2008. Makassar Strait throughflow, 2004 to 2006. Geophys. Res. Lett. 35 (24) https://doi.org/10.1029/2008GL036372.
Hasenfratz, A.P., Jaccard, S.L., Martínez-García, A., Sigman, D.M., Hodell, D.A., Vance, D., Bernasconi, S.M., Kleiven, H.K.F., Haumann, F.A., Haug, G.H., 2019. The residence time of Southern Ocean surface waters and the 100,000-year ice age cycle. Science 363 (6431), 1080–1084. https://doi.org/10.1126/Science.Aat7067.
Herbert, T.D., Lawrence, K.T., Tzanova, A., Peterson, L.C., Caballero-Gill, R., Kelly, C.S., 2016. Late Miocene global cooling and the rise of modern ecosystems. Nat. Geosci. 9 (11), 843–847.
Hodell, D.A., Channell, J.E., Curtis, J.H., Romero, O.E., Röhl, U., 2008. Onset of "Hudson Strait" Heinrich events in the eastern North Atlantic at the end of the middle Pleistocene transition (~ 640 ka)? Paleoceanography 23 (4). https://doi.org/10.1029/2008PA001591.
Hodell, D.A., Charles, C.D., Curtis, J.H., Mortyn, P.G., Ninnemann, U.S., Venz, K.A., 2003. Data report: oxygen isotope stratigraphy of ODP Leg 177 Sites 1088, 1089, 1090, 1093, and 1094. In: Proc. Ocean Drill. Program Sci. Results 177, pp. 1–26.

Holbourn, A., Kuhnt, W., Xu, J., 2011. Indonesian Throughflow variability during the last 140 ka: The Timor Sea outflow. Geological Society, London, Special Publications 355 (1), 283–303.
Itaki, T., 2016. Transitional changes in microfossil assemblages in the Japan Sea from the Late Pliocene to early Pleistocene related to global climatic and local tectonic events. Progr. Earth Planet. Sci. 3 (1), 1–21. https://doi.org/10.1186/s40645-016-0087-4.
Kucera, M., 2003. In: Numerical approach to microfossil proxy data. Lecture notes for Summer School Paleoceanography: theory and field evidence. IAMC Geomare 2003, pp. 66–90.
Le Bars, D., Dijkstra, H.A., De Ruijter, W.P.M., 2013. Impact of the Indonesian Throughflow on Agulhas leakage. Ocean Sci. 9 (5), 773–785. https://doi.org/10.5194/os-9-773-2013.
Lisiecki, L.E., Raymo, M.E., 2005. A Pliocene-Pleistocene stack of 57 globally distributed benthic δ18O records. Paleoceanography 20 (1).
Lutjeharms, J.R.E., 1996. The exchange of water between the South Indian and South Atlantic Oceans. In: The South Atlantic. Springer, Berlin, Heidelberg, pp. 125–162.
Marino, G., Zahn, R., Ziegler, M., Purcell, C., Knorr, G., Hall, I.R., Ziveri, P., Elderfield, H., 2013. Agulhas salt-leakage oscillations during abrupt climate changes of the Late Pleistocene. Paleoceanography 28 (3), 599–606.
Martínez-Garcia, A., Rosell-Melé, A., Jaccard, S.L., Geibert, W., Sigman, D.M., Haug, G. H., 2011. Southern Ocean dust–climate coupling over the past four million years. Nature 476 (7360), 312–315. https://doi.org/10.1038/nature10310.
Martínez-Garcia, A., Rosell-Melé, A., McClymont, E.L., Gersonde, R., Haug, G.H., 2010. Subpolar link to the emergence of the modern equatorial Pacific cold tongue. Science 328 (5985), 1550–1553. https://doi.org/10.1126/science.1184480.
Martínez-Garcia, A., Rosell-Melé, A., McClymont, E.L., Gersonde, R., Haug, G.H., 2010. Subpolar link to the emergence of the modern equatorial Pacific cold tongue. Science 328 (5985), 1550–1553.
Martínez-Méndez, G., Zahn, R., Hall, I.R., Peeters, F.J., Pena, L.D., Cacho, I., Negre, C., 2010. Contrasting multiproxy reconstructions of surface ocean hydrography in the Agulhas Corridor and implications for the Agulhas Leakage during the last 345,000 years. Paleoceanography 25 (4). https://doi.org/10.1029/2009PA001879.
McManus, J.F., Oppo, D.W., Cullen, J.L., 1999. A 0.5-million-year record of millennial-scale climate variability in the North Atlantic. Science 283 (5404), 971–975.
Mohan, K., Gupta, A.K., Bhaumik, A.K., 2011. Distribution of deep-sea benthic foraminifera in the Neogene of Blake Ridge, NW Atlantic Ocean. J. Micropalaeontol. 30, 33–74. https://doi.org/10.1144/0262-821X10-008.
Mortyn, P.G., Charles, C.D., 2003. Planktonic foraminiferal depth habitat and δ18O calibrations: Plankton tow results from the Atlantic sector of the Southern Ocean. Paleoceanography 18 (2).
Nirmal, B., Mohan, K., Prakasam, M., Tripati, A., Mortyn, P.G., Rodríguez-Sanz, L., 2021. Pleistocene surface-ocean changes across the Southern subtropical front recorded by cryptic species of Orbulina universa. Mar. Micropaleontol. 168, 102056 https://doi.org/10.1016/j.marmicro.2021.102056.
Nuber, S., Rae, J., Andersen, M., Zhang, X., de Boer, B., Dumont, M., Sun, Y., Mithan, H., Hall, I., Barker, S., 2021. SeaLevel controls on Agulhas Leakage Salinity and the Atlantic Overturning Circulation.
Peeters, F.J., Acheson, R., Brummer, G.J.A., De Ruijter, W.P., Schneider, R.R., Ganssen, G.M., Ufkes, E., Kroon, D., 2004. Vigorous exchange between the indian and Atlantic oceans at the end of the past five glacial periods. Nature 430 (7000), 661. https://doi.org/10.1038/nature02785.
Petrick, B., Martínez-García, A., Auer, G., Reuning, L., Auderset, A., Deik, H., Takayanagi, H., De Vleeschouwer, D., Iryu, Y., Haug, G.H., 2019. Glacial Indonesian throughflow weakening across the mid-pleistocene climatic transition. Sci. Rep. 9 (1), 1–13. https://doi.org/10.1038/s41598-019-53382-0.
Petrick, B., McClymont, E.L., Littler, K., Rosell-Melé, A., Clarkson, M.O., Maslin, M., Röhl, U., Shevenell, A.E., Pancost, R.D., 2018. Oceanographic and climatic evolution of the southeastern subtropical Atlantic over the last 3.5 Ma. Earth Planet. Sci. Lett. 492, 12–21. https://doi.org/10.1016/j.epsl.2018.03.054.
Rahmstorf, S., 2002. Ocean circulation and climate during the past 120,000 years. Nature 419 (6903), 207–214.
Raymo, M.E., Lisiecki, L.E., Nisancioglu, K.H., 2006. Plio-Pleistocene ice volume, Antarctic climate, and the global δ18O record. Science 313 (5786), 492–495. https://doi.org/10.1126/science.1123296.
Reid, J.L., 1989. On the total geostrophic circulation of the South Atlantic Ocean: flow patterns, tracers, and transports. Prog. Oceanogr. 23 (3), 149–244.
Schiebel, R., Hemleben, C., 2017. Planktic Foraminifers in the Modern Ocean. Springer, Berlin.
Schott, F.A., Xie, S.P., McCreary Jr., J.P., 2009. Indian Ocean circulation and climate variability. Rev. Geophys. 47 (1) https://doi.org/10.1029/2007RG000245.
Simon, M.H., Arthur, K.L., Hall, I.R., Peeters, F.J., Loveday, B.R., Barker, S., Ziegler, M., Zahn, R., 2013. Millennial-scale Agulhas current variability and its implications for salt-leakage through the Indian-Atlantic Ocean Gateway. Earth Planet. Sci. Lett. 383, 101–112.
Speich, S., Blanke, B., De Vries, P., Drijfhout, S., Döös, K., Ganachaud, A., Marsh, R., 2002. Tasman leakage: a new route in the global ocean conveyor belt. Geophys. Res. Lett. 29 (10), 55-1.
Sun, Y., An, Z., Clemens, S.C., Bloemendal, J., Vandenberghe, J., 2010. Seven million years of wind and precipitation variability on the Chinese Loess Plateau. Earth Planet. Sci. Lett. 297 (3–4), 525–535. https://doi.org/10.1016/j.epsl.2010.07.004.
Tolderlund, D.S., 1971. In: Distribution and ecology of living planktonic foraminifera in surface waters of the Atlantic and Indian Oceans.The micropaleontology of oceans, pp. 105–149.
Turney, C.S., Jones, R.T., 2010. Does the Agulhas current amplify global temperatures during super-interglacials? J. Quat. Sci. 25 (6), 839–843. https://doi.org/10.1002/jqs.1423.
Venz, K.A., Hodell, D.A., 2002. New evidence for changes in Plio-Pleistocene deep water circulation from Southern Ocean ODP Leg 177 Site 1090. Palaeogeogr. Palaeoclimatol. Palaeoecol. 182 (3), 197–220.
Zhang, T., Wang, W., Xie, Q., Chen, L., 2019. Heat contribution of the Indonesian throughflow to the Indian Ocean. Acta Oceanol. Sin. 38 (4), 72–79. https://doi.org/10.1007/s13131-019-1414-6.